THE JOURNAL OF BIOLOGICAL CHEMISTRY VOL. 290, NO. 37, pp. 22805–22817, September 11, 2015

Dual Role of Superoxide Dismutase 2 Induced in Activated Microglia

*OXIDATIVE STRESS TOLERANCE AND CONVERGENCE OF INFLAMMATORY RESPONSES**

Received for publication, April 14, 2015, and in revised form, July 28, 2015 Published, JBC Papers in Press, July 31, 2015, DOI 10.1074/jbc.M115.659151

Yasuhiro Ishihara[‡1], Takuya Takemoto[‡], Kouichi Itoh[§], Atsuhiko Ishida[‡], and Takeshi Yamazaki[‡]

From the [‡]Laboratory of Molecular Brain Science, Graduate School of Integrated Arts and Sciences, Hiroshima University, Higashi-Hiroshima 739-8521, Japan and the [§]Laboratory for Brain Science, Kagawa School of Pharmaceutical Sciences, Tokushima Bunri University, Kagawa, 769-2193, Japan

Background: The redox state can affect the proinflammatory responses of microglia.
Results: Superoxide dismutase 2 (SOD2) knockdown in activated microglia increased the production of reactive oxygen species (ROS) as well as inflammatory cytokines.
Conclusion: SOD2 negatively regulates the inflammatory cytokine expression via ROS elimination.
Significance: Our findings demonstrate a novel mechanism regulating microglial proinflammatory responses via oxidative stress.

Microglia are activated quickly in response to external pathogens or cell debris and clear these substances via the inflammatory response. However, excessive activation of microglia can be harmful to host cells due to the increased production of reactive oxygen species and proinflammatory cytokines. Superoxide dismutase 2 (SOD2) is reportedly induced under various inflammatory conditions in the central nervous system. We herein demonstrated that activated microglia strongly express SOD2 and examined the role of SOD2, focusing on regulation of the microglial activity and the susceptibility of microglia to oxidative stress. When rat primary microglia were treated with LPS, poly(I:C), peptidoglycan, or CpG oligodeoxynucleotide, respectively, the mRNA and protein levels of SOD2 largely increased. However, an increased expression of SOD2 was not detected in the primary neurons or astrocytes, indicating that SOD2 is specifically induced in microglia under inflammatory conditions. The activated microglia showed high tolerance to oxidative stress, whereas SOD2 knockdown conferred vulnerability to oxidative stress. Interestingly, the production of proinflammatory cytokines was increased in the activated microglia treated with SOD2 siRNA compared with that observed in the control siRNA-treated cells. Pretreatment with NADPH oxidase inhibitors, diphenylene iodonium and apocynin, decreased in not only reactive oxygen species generation but also the proinflammatory cytokine expression. Notably, SOD2 knockdown largely potentiated the nuclear factor κB activity in the activated microglia. Taken together, increased SOD2 conferred tolerance to oxidative stress in the microglia and decreased proinflammatory cytokine production by attenuating the nuclear factor κB activity. Therefore, SOD2 might regulate neuroinflammation by controlling the microglial activities.

Microglia constitute the primary immune cells of the central nervous system (CNS) and are activated quickly in response to external pathogens or cell debris, after which they act by releasing inflammatory factors and/or engulfing foreign bodies to mediate the inflammatory response. However, excessive activation of microglia may be harmful to host cells; for example, microglia can promote the development of various neuronal diseases by producing large amounts of inflammatory molecules, such as tumor necrosis factor-α (TNFα), interleukin-1β (IL-1β), and reactive oxygen species (ROS).[2] Indeed, microglia with abnormal activity reportedly induce neuroinflammation and are implicated in the pathogenesis of Parkinson disease, Alzheimer disease, brain ischemia-reperfusion injury, trauma, epilepsy, depression, and schizophrenia (1–5). Therefore, understanding the mechanisms that control the microglial activity is critical, not only for comprehending the physiology of microglia but also for developing new therapeutic approaches to treating neuroinflammation and/or neurodegenerative diseases.

The main source of ROS in microglia is NADPH oxidase (6). NADPH oxidase is a multisubunit enzyme complex that transfers electrons to molecular oxygen from NADPH or, to a lesser extent, NADH (7), resulting in the formation of superoxide anions as the primary product. Earlier investigations have demonstrated the relevant role of NADPH oxidase in the acute inflammatory response induced by neutrophils, with evidence showing its participation in respiratory

* This work was supported in part by KAKENHI Grants 26740024, 30291149, and 22310041 from the Ministry of Education, Culture, Sports, Science, and Technology of Japan (to Y. I., K. I., and T. Y.); a grant from the Fujii Foundation (to Y. I.); and a grant from the Hiroshima University Education and Research Support Foundation (to Y. I.). The authors declare that they have no conflicts of interest with the contents of this article.

[1] To whom correspondence should be addressed: Laboratory of Molecular Brain Science, Graduate School of Integrated Arts and Sciences, Hiroshima University, 1-7-1, Kagamiyama, Higashi-Hiroshima, Hiroshima 739-8521, Japan. Tel.: 81-82-424-6500; Fax: 81-82-424-0759; E-mail: ishiyasu@hiroshima-u.ac.jp.

[2] The abbreviations used are: ROS, reactive oxygen species; AP-1, activator protein-1; DHE, dihydroethidium; DPI, diphenylene iodonium; MAP2, microtubule-associated protein 2; MCP-1, monocyte chemotactic protein-1; NF-κB, nuclear factor κB; PGN, peptidoglycan(s); SOD2, superoxide dismutase 2; TLR, toll-like receptor; CAPE, caffeic acid phenylethyl ester; ANOVA, analysis of variance.

bursts killing pathogens (8, 9). Mitochondria are another source of ROS inside activated microglia. Copper chloride has been shown to stimulate mitochondrial superoxide production in murine BV-2 microglial cells (10). Lipopolysaccharide (LPS), an endotoxin found in the outer membrane of Gram-negative bacteria, also elicits mitochondrial superoxide production, which is regulated by the mitochondrial chaperone glucose-regulated protein 75 (Grp75/mortalin) (11). Naik and Dixit (12) suggested that alterations in the redox environment of the plasma membrane could cause mitochondrial ROS formation. Therefore, ROS derived from NADPH oxidase are closely linked to mitochondrial ROS production.

Proinflammatory cytokines and chemokines are transcriptionally activated by several inflammatory transcription factors, including activator protein-1 (AP-1) and nuclear factor κB (NF-κB), that act downstream of pattern-recognition receptors, such as Toll-like receptors (TLRs) in microglia. Growing evidence has shown that the ROS generated within microglia can increase the expression of proinflammatory mediators, suggesting that ROS are a modulator of microglial activation. Indeed, LPS, interferon γ, and amyloid β(1–42) stimulate ROS production by NADPH oxidase, especially NOX1, NOX2, and NOX4, and increases in ROS subsequently induce the expression of several proinflammatory molecules, such as TNFα, IL-1β, inducible nitric-oxide synthase, prostaglandin E2, and monocyte chemotactic protein-1 (MCP-1) (13–18). Furthermore, the antioxidant molecule α-tocopherol has been reported to decrease the levels of proinflammatory and adhesion molecules and elicit microglial ramification by scavenging ROS (19–22). Therefore, the redox balance is thought to regulate a series of neuroinflammatory processes mediated by microglia.

Superoxide dismutase (SOD) is a major antioxidant enzyme in aerobic organisms and dismutates superoxide anions to form hydrogen peroxide and molecular oxygen. SOD1 (Cu/Zn-SOD) is present in the cytoplasm, nucleus, and peroxisomes of all mammalian cells, where it scavenges superoxide. SOD2 (Mn-SOD) is localized within mitochondria and efficiently eliminates the superoxide generated from molecular oxygen in the respiratory chain. SOD2 is reportedly induced in the CNS under inflammatory conditions. Notably, the intraventricular injection of LPS has been shown to increase the SOD2 expression in the whole brains of rats (23), and treatment of mesencephalic cultures with LPS has been demonstrated to elicit SOD2 expression, probably in astrocytes (24). Moreover, there are a few reports in which mouse primary microglia or the murine microglial cell line, BV-2, showed an increased expression of SOD2 after treatment with LPS (25, 26), and inducible SOD2 is thought to attenuate oxidative injury (25, 27). However, if the redox environment regulates microglial inflammatory processes, SOD2 might also modulate the microglial activity. In this study, we demonstrated that activated microglia strongly express SOD2. We then examined the role of the SOD2 induced in microglia, focusing on the sensitivity of these cells to oxidative stress as well as regulation of the microglial activity.

Experimental Procedures

Materials—LPS from *Escherichia coli* 026:B6, peptidoglycan (PGN), SP600125, acetyl cytochrome *c*, xanthine oxidase, and diphenylene iodonium (DPI) were obtained from Sigma-Aldrich. U0126 and hydrogen peroxide were purchased from Wako Pure Chemical Industries, Ltd. (Osaka, Japan). Poly(I:C) was obtained from Tocris (Minneapolis, MN). Caffeic acid phenylethyl ester (CAPE) was purchased from Cayman Chemical (Ann Arbor, MI). Dihydroethidium (DHE) was purchased from Molecular Probes, Inc. (Eugene, OR). Apocynin was purchased from Nacalai Tesque (Kyoto, Japan). Xanthine was obtained from Merck Millipore. Single-stranded DNA molecules containing unmethylated CpG dinucleotides (CpG DNA) were synthesized by Eurofins Genomics (Huntsville, AL). WP9QY was purchased from AnaSpec, Inc. (Fremont, CA). IL-1RA was obtained from Bioworld Technology (St. Louis Park, MN). All other chemicals were obtained from Wako Pure Chemical Industries or Sigma-Aldrich and were of reagent grade.

Animals—All animal procedures were performed in accordance with the Fundamental Guidelines for Proper Conduct of Animal Experiments and Related Activities in Academic Research Institutions under the jurisdiction of the Ministry of Education, Culture, Sports, Science, and Technology (Tokyo, Japan) and the Animal Care and Use Committee of Hiroshima University (Hiroshima, Japan). Pregnant Wistar rats and male ICR mice were obtained from Kyudo (Kumamoto, Japan) and maintained in a temperature-controlled animal facility with a 12-h light/dark cycle.

Isolation and Culture of Rat Primary Microglia—Cultures of primary microglia were prepared from 1–3-day-old Wistar rats, according to our previous report (28). Briefly, the forebrain was dissociated, and the cells were plated in a poly-L-lysine-coated plastic culture flask with tissue culture medium, which consisted of Dulbecco's modified Eagle's medium (DMEM) supplemented with 10% fetal bovine serum (FBS) and 5 μg/ml insulin. After 9–12 days, microglia were harvested by shaking the flask and seeded at a density of 1×10^5 cells/cm^2. The culture medium was changed to remove non-adherent cells 30 min after seeding. The cultures of isolated microglia were uniformly immunopositive for CD11b and contained >95% microglial cells.

Total RNA Extraction and Real-time PCR—Determination of the mRNA levels was performed according to our previous report (29). The primer sequences are shown in Table 1. The amount of mRNA was normalized to that of glyceraldehyde-3-phosphate dehydrogenase (GAPDH), and the values for the treated samples were divided by those for the untreated samples to calculate the relative mRNA levels.

Immunoblotting—Microglia were collected and lysed with radioimmune precipitation assay buffer (25 mM Tris-HCl, pH 7.6, 150 mM NaCl, 1% Nonidet P-40, 1% sodium deoxycholate, and 0.1% SDS). Equal amounts of protein were loaded and separated via SDS-PAGE using 10 or 12% (w/v) polyacrylamide gels and then transferred onto polyvinylidene difluoride membranes. The blocked membranes were incubated with the following primary antibodies: anti-SOD2 (ADI-SOD-111 rabbit, Enzo Life Sciences, Farmingdale, NY) and anti-α-tubulin

TABLE 1
List of rat primers for real-time PCR used in this study

	Forward (5′–3′)	Reverse (5′–3′)
TNFα	AGCCCTGGTATGAGCCCATGTA	CCGGACTCCGTGATGTCTAAGT
IL-1β	CACCTCTCAAGCAGAGCACAGA	ACGGGTTCCATGGTGAAGTC
COX-2	TTTGTTGAGTCATTCACCAGACAGAT	ACGATGTGTAAGGTTTCAGGGAGAAG
MCP-1	TGTCTCAGCCAGATGCAGTT	CAGCCGACTCATTGGGATCA
MIP-2α	CCCTCCTGTGCTCAAGACTC	CCACAACAACCCCTGTACCC
SOD1	TTCGAGCAGAAGGCAAGCGGTG	TCTTCATCCGCTGGACCGCCA
SOD2	GCGCTGGCCAAGGGAGATGTT	ATGGCCCCCGCCATTGAACTT
Catalase	CGTGCTCGCGTGGCCAACTA	AGTTGGGAGCACCACCCTGGT
GPx1	TCGGACATCAGGAGAATGGCAAGAA	GCTGGCAAGGCATTCCGCAG
Glutathione reductase	GTGGTCTTCAGCCACCCGCC	ATCGGGGTGAAGGCGGTCGA
Thioredoxin reductase	TCCGTCAGGCCTCGCATCCA	CCGCCGCCCTATGAGCAAGG
GAPDH	AACGACCCCTTCATTGACCT	CCTTGACTGTGCCGTTGAACT

(T5168 mouse, Sigma-Aldrich). Finally, the membranes were incubated in solutions of peroxide-conjugated secondary antibodies (Thermo Fisher Scientific) and then visualized using peroxide substrates (SuperSignal West Femto, Thermo Fisher Scientific). The band intensity was quantified using the ImageJ software program (National Institutes of Health, Bethesda, MD).

Culture of Rat Primary Cortical Neurons—Rat primary cortical neurons were prepared from Wistar rats on the 17th day of gestation, as reported previously with minor modifications (30). The cortex was separated, and the meninges were removed. The tissues were cut into small pieces and then dissociated using a papain dissociation system (Worthington). The resulting cell suspension was filtered through a cell strainer (40 μm, Falcon) and plated on polyethyleneimine-coated dishes at a density of 5×10^5 cells/ml with Neurobasal medium and B27 supplement (Gibco). After 2 days of culture, cytosine β-D-arabinofuranoside was added to inhibit glial proliferation (final concentration, 1 μM), and the medium was changed completely after 2 days to remove the cytosine β-D-arabinofuranoside. The purity of the neurons was assayed using microtubule-associated protein 2 (MAP2) staining, and >95% of cells in the culture showed MAP2 immunoreactivity (Fig. 3*A*).

Culture of Rat Primary Cortical Astrocytes—Cultures of primary astrocytes were prepared from the cerebral cortex of 1–2-day-old male Wister rats (31). The cerebral hemispheres were excised, and the meninges were removed. The cerebral cortex was cut into small pieces and treated with 2.5% trypsin and 0.5% DNase I for 20 min at 37 °C. The cells then were plated at a density of 8×10^5 cells/well in 6-well plates coated with poly-L-lysine using DMEM containing 10% FBS. The medium was changed every 2 days after shaking the plates at 250 rpm to remove other glial cells. Finally, the purity of the astrocyte-enriched cultures was confirmed by staining with antibodies against the astrocyte-specific marker, glial fibrillary acidic protein, and >95% of the cultured astrocytes showed immunoreactivity to glial fibrillary acidic protein (Fig. 3*A*).

RNA Interference—SOD2 siRNAs included three selected siRNA constructs against rat SOD2, provided by the Invitrogen Stealth Select RNAi library (Invitrogen). The catalogue numbers of the constructs are RSS302728, RSS302727, and RSS302729. A mixture of two control siRNAs (12935-300 and 12935-200, Invitrogen) was used as a control. SOD2 siRNA and control siRNA were transfected into primary microglial cells using Lipofectamine 2000 reagent (Invitrogen), as recommended by the manufacturer. The cells were used in further experiments 24 h after transfection.

Measurement of the ROS Levels—ROS generated inside the microglia were detected with DHE, a fluorescent dye, according to our previous method, with slight modifications (32). Cells were treated with 10 μM DHE for 10 min in a humidified CO_2 incubator at 37 °C. Fluorescent images were obtained using a BZ-9000 inverted fluorescent microscope (Keyence, Osaka, Japan) at 540 ± 25-nm excitation, with a 605 ± 55-nm band pass filter.

The amount of superoxide anion produced by the microglia was quantified using acetylated cytochrome *c* (33). Briefly, 60 μM acetylated cytochrome *c* was added to the culture and incubated for another 5 min in the presence of 100 μM diethyldithiocarbamate and 100 units/ml of catalase. The amount of reduced acetylated cytochrome *c* was determined based on the difference in absorbance between 550 and 557 nm. The total amount of superoxide anions in the culture medium was calculated using the absorption coefficient of reduced acetylated cytochrome *c* ($\epsilon_{550-557} = 21.0\ \mathrm{mM}^{-1}\ \mathrm{cm}^{-1}$).

Measurement of Cell Viability—The degree of cell viability was determined by comparing the percentage of the lactate dehydrogenase activity in the medium and cell lysates, according to our previous report (33).

Cloning and Site-directed Mutagenesis of the Rat SOD2 Promoter Region—Rat genomic DNA was extracted from rat whole brains using the DNeasy blood and tissue kit (Qiagen, Valencia, CA). The SOD2 promoter region (1,267 bp) was amplified with Platinum *Taq* DNA polymerase high fidelity (Invitrogen; primers: 5′-CAGGAACAGCCACTACAGTAT-3′ (forward) and 5′-ACCGCTGCTCTCCTCAGAA-3′ (reverse)) and ligated into pGL4.24 to create pGL4.24-SOD2Prom, which contains a SOD2Prom-luc transcriptional fusion. Mutation of the AP-1 and NF-κB binding sites in pGL4.24-SOD2Prom was performed via site-directed mutagenesis using the QuikChange kit (Stratagene, Santa Clara, CA; primers: AP-1 Se, 5′-CAGGGCATAAATTAAGTGAGTTGGAAGGACCCTG-3′; NF-κB Se, 5′-GGAGGAAAGTCTCCGCCGCTTTCCAGAACCAGG-3′); the mutants were named pGL4.24-SOD2Prom AP-1m, pGL4.24-SOD2Prom NF-κBm, and pGL4.24-SOD2Prom AP-1m NF-κBm, respectively.

Luciferase Assay—The constructs of pGL4.24-SOD2Prom, pGL4.24-SOD2Prom AP-1m, pGL4.24-SOD2Prom NF-κBm, pGL4.24-SOD2Prom AP-1m NF-κBm, and pNL3.2.NF-κB-RE (Promega, Madison, WI) were transfected into rat primary

TABLE 2
List of mouse primers for real-time PCR used in this study

	Forward (5′–3′)	Reverse (5′–3′)
TNFα	ATGGCCTCCCTCTCATCAGT	CTTGGTGGTTTGCTACGACG
IL-1β	AGCTTCCTTGTGCAAGTGTCT	GCAGCCCTTCATCTTTTGGG
SOD2	GTGTCTGTGGGAGTCCAAGG	AGCGGAATAAGGCCTGTTGT
β-Actin	CTAGGCACCAGGGTGTGATG	GGGGTACTTCAGGGTCAGGA

microglia using Lipofectamine 2000 (Invitrogen) according to the manufacturer's instructions. Twenty-four hours after transfection, the cells were used in the experiments. The luciferase activity was measured using the Luciferase Assay System (Promega) for the pGL4 vector or the Nano-Glo Luciferase Assay System (Promega) for the pNL vector with a GloMax 20/20 Luminometer (Promega).

Enzyme-linked Immunosorbent Assay—The levels of TNFα and IL-1β in the culture supernatants of the microglia were evaluated using the TNFα and IL-1β Mini ELISA Development Kit (PeproTech, Rocky Hill, NJ), according to the manufacturer's instructions.

Evaluation of the NF-κB Binding Activity—Nuclear extracts were prepared according to our previous report with slight modifications (34). Briefly, cells were suspended in buffer A (10 mM HEPES, pH 7.8, 10 mM KCl, 2 mM $MgCl_2$, 0.1 mM EDTA, 0.5 mM DTT, and protease inhibitor mixture) and incubated on ice for 15 min. Nonidet P-40 at a final concentration of 0.6% was added to the cell suspension, which was immediately vortexed and centrifuged. The resulting white pellets were washed with buffer A, and nuclear proteins were extracted with buffer B (50 mM HEPES, pH 7.8, 50 mM KCl, 300 mM NaCl, 0.1 mM EDTA, 0.5 mM DTT, 10% (v/v) glycerol). The specific DNA binding activity of NF-κB p65 was measured using the NF-κB (p65) transcription factor assay kit (Cayman Chemical), according to the manufacturer's instructions.

Intracerebroventricular Injection of LPS—Eight-week-old male ICR mice were initially anesthetized for surgery using a mixture of 1.5–2.0% isoflurane (160 ml/min, Wako) and oxygen. The head was skinned, and a 27-gauge injection needle was inserted into the cerebroventricular region (anterior, 0.5 mm; lateral, 1.0 mm; ventral, 5.0 mm from bregma). LPS was injected at a volume of 2 μl over 2 min using a Hamilton syringe, and the needle was left in place for an additional 1 min. The mice were killed 3 h after injection. RNA was extracted from the cerebral cortex, and the cDNA was synthesized via RT-PCR, followed by real-time PCR using the specific primers listed in Table 2.

Statistical Analyses—All data are expressed as the means ± S.E. The statistical analyses were performed using a one-way analysis of variance (ANOVA), followed by Student's *t* test or Dunnett's test. The Holm or Bonferroni methods were used to correct for multiple comparisons. *p* values of <0.05 were considered to be statistically significant.

Results

SOD2 Up-regulation Occurs Downstream of TLRs in Microglia—When the rat primary microglia were stimulated with LPS for 6 h, the mRNA expression of proinflammatory molecules, such as TNFα, IL-1β, COX-2 (cyclooxygenase-2), MCP-1, and MIP-2α (macrophage inflammatory protein-2α), was largely increased (Fig. 1*A*), clearly indicating the induction of microglial activation by LPS. Interestingly, the activated microglia strongly expressed SOD2 mRNA, compared with the unstimulated cells, whereas the expression of the other antioxidant enzymes, SOD1, catalase (*Cat*), glutathione reductase (*GR*), and thioredoxin reductase (*TR*), remained unchanged in the presence of LPS (Fig. 1*B*). The expression of glutathione peroxidase 1 (*GPx1*) slightly decreased by LPS (Fig. 1*B*). The time course of the changes in the SOD2 mRNA expression was almost the same as that for the proinflammatory cytokines, TNFα and IL-1β; namely, the SOD2 mRNA levels started to increase 1 h after LPS treatment, reached a peak at 6 h, and then slightly decreased (Fig. 1*C*). The protein levels of SOD2 also increased 1 h after LPS treatment, and a prolonged increment was observed during 24 h of incubation of the microglia with LPS (Fig. 1*D*).

To date, more than 10 functional TLRs have been identified in humans and rodents (35) and are expressed in a variety of cells, including microglia. We stimulated rat primary microglia with major TLR ligands other than LPS, including poly(I:C) as a ligand for TLR3, PGN as a ligand for TLR6, and synthetic CpG DNA as a ligand for TLR9. Poly(I:C), PGN, and CpG DNA increased the mRNA expression of TNFα and IL-1β in the primary microglia (Fig. 2*A*), indicating that the microglia were also activated by these TLR ligands. The effect of CpG DNA on microglial activation was less pronounced than that of the other TLR ligands. Remarkably, poly(I:C), PGN, and CpG DNA elicited an increased expression of SOD2 mRNA as well as SOD2 proteins (Fig. 2*B*). A TLR4 antagonist, TAK-242, clearly suppressed the mRNA expression of TNFα, IL-1β, and SOD2 induced by LPS (Fig. 2*C*), indicating that the increased expression of TNFα, IL-1β, and SOD2 was elicited downstream of TLR4. The transcriptional activation of SOD2 has been reported in response to several proinflammatory cytokines (36, 37). However, the TNF receptor antagonist WP9QY and IL-1 receptor antagonist IL-1RA did not have an effect on the SOD2 expression induced by LPS (Fig. 2*D*). These data indicate that the SOD2 expression is induced downstream of TLRs, which is independent of TNFα and IL-1β signaling.

We examined whether SOD2 may be induced in other cells in the CNS, such as neurons and astrocytes. In primary neurons, the expression of TNFα, IL-1β, and SOD2 was not affected by LPS treatment for 24 h (Fig. 3*B*). Additionally, the primary astrocytes showed an increased expression of TNFα and IL-1β mRNA at early time points; however, no changes were noted in the mRNA levels of SOD2 following treatment with LPS during the experiments (Fig. 3*C*). Therefore, SOD2 induction downstream of TLRs can be considered specific to microglia in the CNS.

Transcription Factors Responsible for the Inducible Expression of SOD2 in Microglia—A promoter analysis revealed that the promoter region of rat SOD2 has NF-κB and AP-1 binding sequences (Fig. 4*A*). Furthermore, because AP-1 and NF-κB have been reported to drive the SOD2 expression (38–41), we next examined the involvement of NF-κB and AP-1 in the SOD2 expression induced by LPS in the rat primary microglia. Pretreatment with an NF-κB inhibitor, CAPE, significantly suppressed not only the mRNA levels of TNFα and IL-1β but

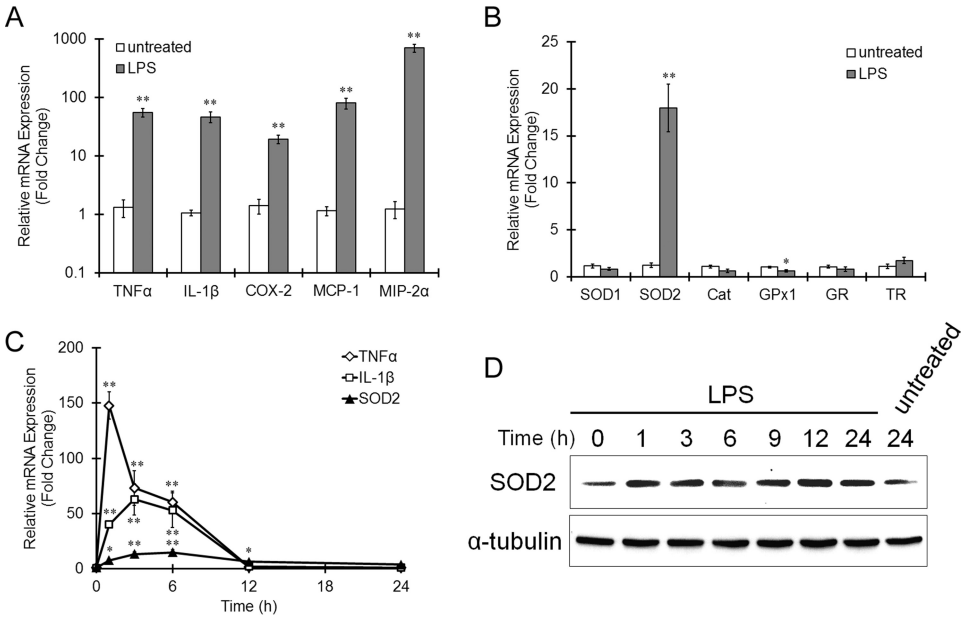

FIGURE 1. **Increased expression of SOD2 in microglia treated with LPS.** Rat primary microglia were stimulated with 10 ng/ml LPS for 24 h. The mRNA levels of proinflammatory molecules TNFα, IL-1β, COX-2, MCP-1, and MIP-2α (*A*) and antioxidant enzymes SOD1, SOD2, catalase (*Cat*), glutathione peroxidase 1 (*GPx1*), glutathione reductase (*GR*), and thioredoxin reductase (*TR*) (*B*) were determined at 6 h using real-time PCR and are represented as -fold changes from the levels measured in untreated cells. The values represent the mean ± S.E. (*error bars*) of 8–14 separate experiments. The data were compared using Student's *t* test. **, $p <$ 0.01 *versus* the untreated cells. *C*, time course of the mRNA expression of TNFα, IL-1β, and SOD2 in the LPS-stimulated microglia. The values represent the mean ± S.E. of five separate experiments. The data were analyzed using one-way ANOVA, followed by Dunnett's test. *, $p < 0.05$; **, $p < 0.01$ *versus* the cells at time 0. *D*, images of immunoblotting showing the protein levels of SOD2 and α-tubulin at 24 h. The results are representative of three independent experiments.

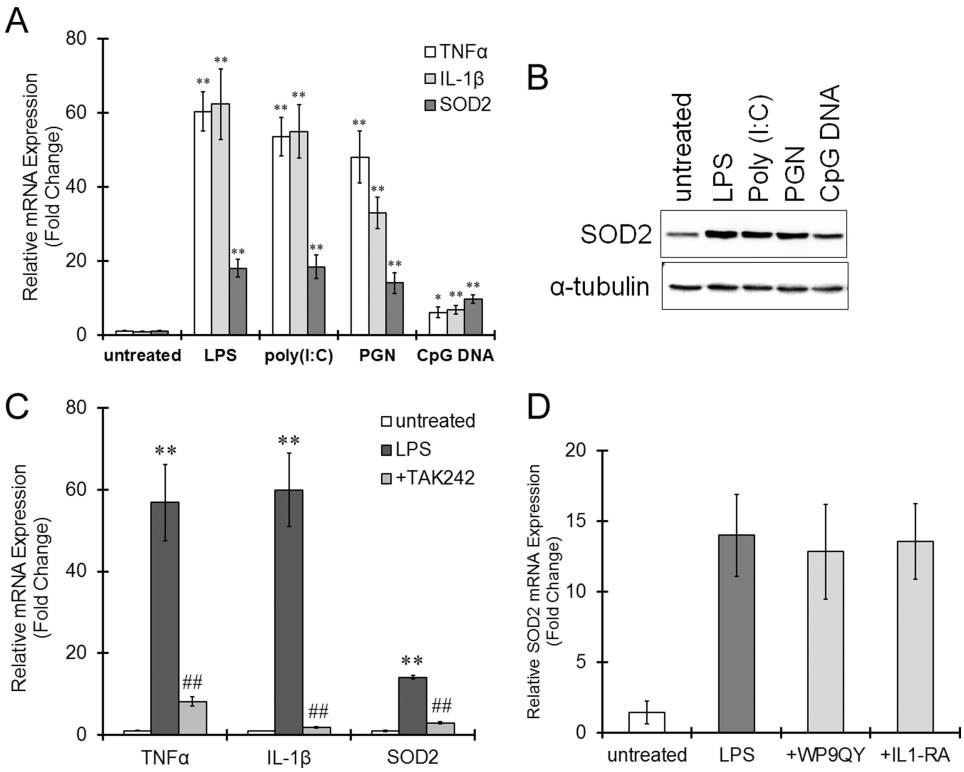

FIGURE 2. **SOD2 expression downstream of TLR stimulation.** *A*, rat primary microglia were treated with 10 ng/ml LPS, 50 μg/ml poly(I:C), 50 μg/ml PGN, or 1 μM CpG DNA for 6 h. The mRNA levels of TNFα, IL-1β, and SOD2 were evaluated using real-time PCR and are represented as -fold change from the levels measured in untreated cells. The values represent the mean ± S.E. (*error bars*) of eight separate experiments. The data were compared using Student's *t* test with Holm's corrections for multiple comparisons. *, $p < 0.05$; **, $p < 0.01$ *versus* the untreated cells. *B*, after 24 h of incubation of microglia with LPS, poly(I:C), PGN, or CpG DNA, the levels of SOD2 and α-tubulin proteins were measured using immunoblotting. The results are representative of three independent experiments. *C*, rat primary microglia were pretreated with a TLR4 antagonist, TAK-242 (1 μM), followed by treatment with 10 ng/ml LPS for 6 h. The levels of TNFα, IL-1β, and SOD2 mRNA were measured using real-time PCR. The values represent the mean ± S.E. of five separate experiments. The data were compared using Student's *t* test with Holm's corrections for multiple comparisons. **, $p < 0.01$ *versus* the untreated cells. ##, $p < 0.01$ *versus* the LPS-treated cells. *D*, rat primary microglia were pretreated with TNFα or IL-1 receptor antagonists (20 μM WP9QY or 1.5 μg/ml IL-1RA, respectively) followed by treatment with 10 ng/ml LPS for 6 h. The levels of SOD2 mRNA were measured using real-time PCR.

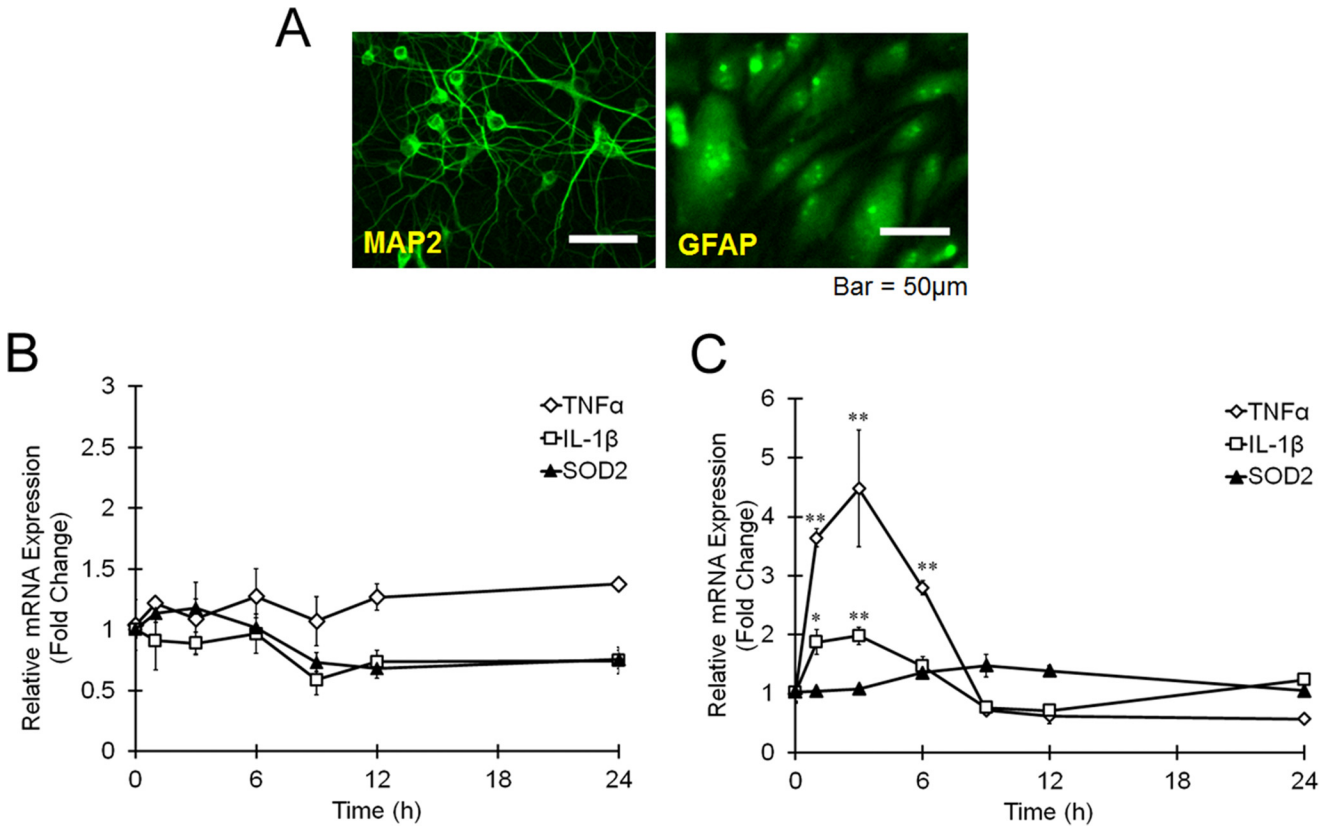

FIGURE 3. **Effects of LPS on the SOD2 expression in primary neurons and astrocytes.** *A*, immunocytochemical staining of rat primary neurons treated with the MAP2 antibody (*left*) and rat primary astrocytes treated with glial fibrillary acidic protein (*GFAP*) (*right*). *B* and *C*, rat primary neurons (*B*) or astrocytes (*C*) were treated with 10 ng/ml LPS for 24 h, and the time course of the mRNA expression of TNFα, IL-1β, and SOD2 was evaluated using real-time PCR. The values represent the mean ± S.E. of 3–5 separate experiments. The data were analyzed using one-way ANOVA, followed by Dunnett's test. *, $p < 0.05$; **, $p < 0.01$ *versus* the cells at time 0.

also the amount of SOD2 mRNA induced by LPS (Fig. 4*B*). Challenges with the MEK1 inhibitor, U0126, and JNK inhibitor, SP600125, also reduced the mRNA expression of TNFα, IL-1β, and SOD2 elicited by LPS (Fig. 4*B*). A luciferase assay using the cloned rat SOD2 promoter region demonstrated that treatment of microglia with LPS transcriptionally activated the luciferase expression, whereas pretreatment with CAPE, U0126, or SP600125 attenuated the luciferase activity induced by LPS (Fig. 4*C*). In addition, mutations targeting the NF-κB and AP-1 binding sequences in the SOD2 promoter significantly suppressed luciferase transactivation (Fig. 4*D*). These results suggest that SOD2 is transcriptionally activated via NF-κB- and AP-1-related pathways downstream of TLRs.

Involvement of Up-regulated SOD2 in the Antioxidant Defenses of Microglia—Because SOD2 is a well known enzyme that scavenges superoxide anions, the most obvious role for the SOD2 induced by LPS is to eliminate the superoxide produced by microglia and attenuate oxidative stress. Therefore, the relationship between an increased expression of SOD2 and oxidative injury in microglia was investigated using the RNAi method. Transfection of SOD2 siRNA clearly suppressed the SOD2 mRNA and protein expression elicited by LPS (Fig. 5, *A–C*). The intracellular ROS levels in the microglia were increased by treatment with LPS (Fig. 5*D*). In SOD2-knockdown microglia, ROS production was clearly potentiated in the presence of LPS (Fig. 5*D*). However, ROS production did not increase in the LPS-treated microglia with SOD2 knockdown to which membrane-permeable SOD (SOD-PEG) was added (Fig. 5*D*), indicating that the SOD2 elicited by treatment with LPS contributes to the elimination of the ROS produced by LPS stimulation. In addition, the extracellular ROS levels were also increased by treatment with LPS, and ROS production was enhanced by the knockdown of SOD2 (Fig. 5*E*). The NADPH oxidase inhibitors, DPI and apocynin, partially but significantly suppressed the potentiated ROS generation noted in SOD2-knockdown cells (Fig. 5*E*), suggesting that the SOD2 up-regulated in response to LPS eliminates the superoxide derived from NADPH oxidase.

Treatment with LPS did not injure microglia carrying control siRNA, whereas the microglia treated with SOD2 knockdown were significantly damaged by LPS, suggesting that SOD2 plays a role in the self-protection of microglia under inflammatory conditions (Fig. 6). When unstimulated microglia were treated with the oxidants, 300 μM hydrogen peroxide or 100 μM xanthine plus 30 milliunits/ml xanthine oxidase for 24 h, cell viability decreased to 41.0 and 36.1%, respectively (Fig. 6). Interestingly, treatment with hydrogen peroxide and xanthine/xanthine oxidase did not induce any reductions in cell viability in the LPS-treated microglia (Fig. 6), demonstrating higher tolerance of the activated microglia to oxidative stress. In contrast, SOD2 knockdown clearly abolished the tolerance of the microglia stimulated with LPS (Fig. 6). Therefore, the SOD2 up-reg-

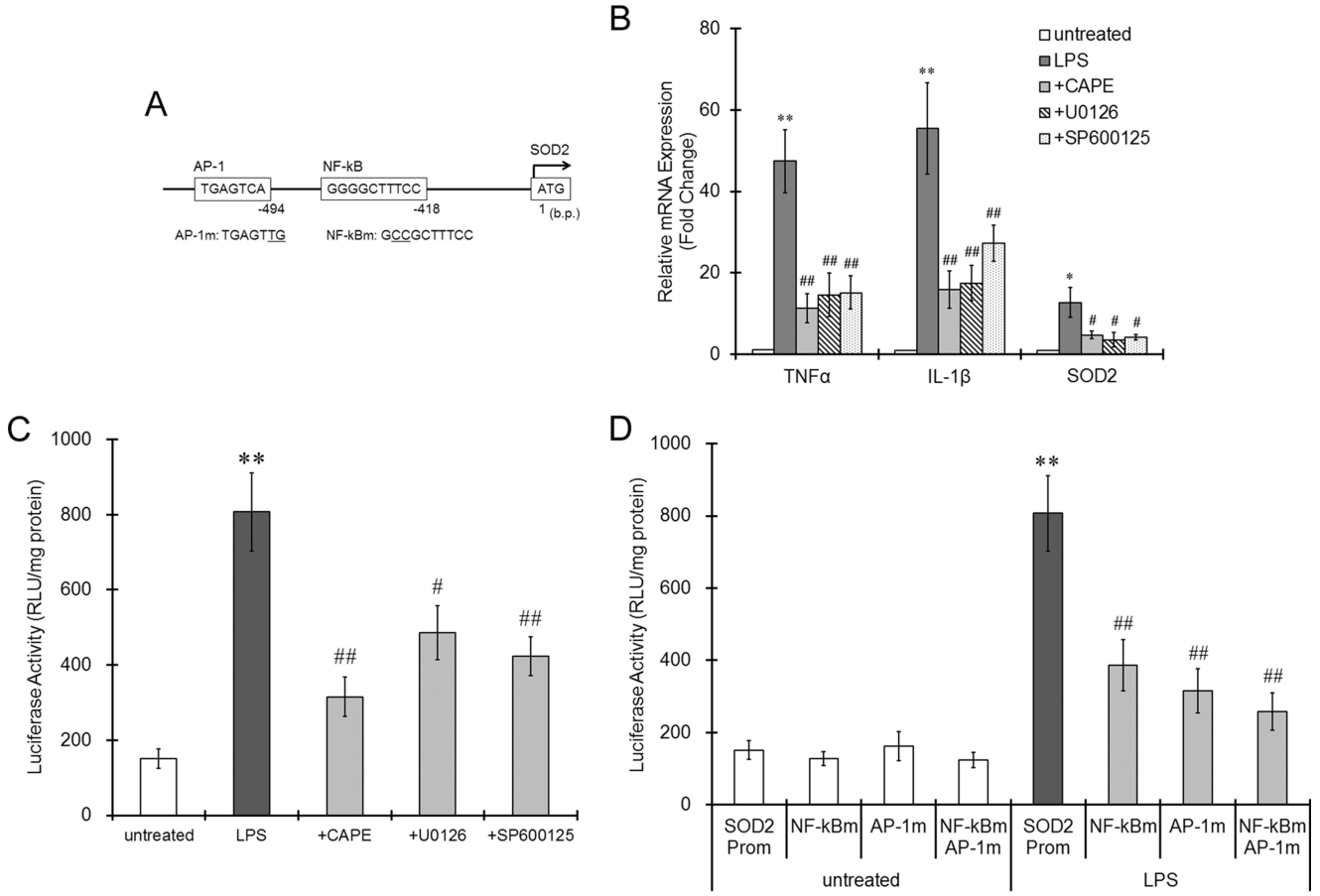

FIGURE 4. **Involvement of NF-κB and AP-1 in the SOD2 expression in activated microglia.** *A*, promoter region of the rat *SOD2* gene. *AP-1m* and *NF-κBm*, mutated sequences of the pGL4.24-SOD2Prom. *B*, rat primary microglia were pretreated with 10 μM CAPE, 10 μM U0126, or 10 μM SP600125 for 20 min and then stimulated with 10 ng/ml LPS for 6 h. The mRNA levels of TNFα, IL-1β, and SOD2 were evaluated using real-time PCR and are represented as -fold changes from the levels measured in untreated cells. The values represent the mean ± S.E. (*error bars*) of six separate experiments. The data were analyzed using one-way ANOVA, followed by Student's *t* test or Dunnett's test. The Bonferroni method was used to correct for multiple comparisons. *, $p < 0.05$; **, $p < 0.01$ *versus* the untreated cells. #, $p < 0.05$; ##, $p < 0.01$ *versus* the LPS-treated cells. *C*, after transfection with pGL4.24-SOD2Prom into rat primary microglia, the cells were cultured for 24 h. The cells were pretreated with 10 μM CAPE, 10 μM U0126, or 10 μM SP600125 for 20 min and then treated with 10 ng/ml LPS and subsequently incubated for 3 h, at which time the luciferase activity was measured. The values represent the mean ± S.E. of 8–10 separate experiments. The data were analyzed using one-way ANOVA, followed by Student's *t* test or Dunnett's test. The Bonferroni method was used to correct for multiple comparisons. **, $p < 0.01$ *versus* the untreated group carrying pGL4.24-SOD2Prom. #, $p < 0.05$; ##, $p < 0.01$ *versus* the LPS-treated group carrying pGL4.24-SOD2Prom. *D*, rat primary microglia were transfected with pGL4.24-SOD2Prom or mutant pGL4.24-SOD2Prom and then cultured for 24 h. The cells were treated with 10 ng/ml LPS for 3 h, followed by measurement of the luciferase activity. The values represent the mean ± S.E. of 8–11 separate experiments. The data were analyzed using one-way ANOVA, followed by Student's *t* test or Dunnett's test. The Bonferroni method was used to correct for multiple comparisons. **, $p < 0.01$ *versus* the untreated group carrying pGL4.24-SOD2Prom; ##, $p < 0.01$ *versus* the LPS-treated group carrying pGL4.24-SOD2Prom.

ulated by LPS confers tolerance to oxidative stress on microglia in order to enhance their survival under conditions of severe oxidative stress, such as inflammation.

Involvement of Increased SOD2 in Suppression of the Inflammatory Cytokine Expression—Of note, we found that the mRNA expression of TNFα and IL-1β 6 h after LPS stimulation was significantly enhanced by SOD2 knockdown, and this enhancement was largely suppressed by pretreatment with the NADPH oxidase inhibitors, DPI and apocynin (Fig. 7*A*). Potentiation of the cytokine expression was also observed in microglia with SOD2 knockdown 12 h after the addition of LPS (Fig. 7*B*), indicating that the proinflammatory response is prolonged by SOD2 knockdown. The levels of TNFα and IL-1β proteins released into the culture medium by the SOD2-knockdown microglia were higher than the levels noted in the medium of the control microglia 24 h after stimulation with LPS (Fig. 7*C*). These data suggest that SOD2 suppresses the cytokine expression to terminate microglial proinflammatory responses.

NF-κB is responsible for the expression of several cytokines under inflammation in the CNS, and ROS are known to regulate the activity of NF-κB (42, 43). Treatment of microglia with ROS or ROS-generating reagents increased the mRNA expression of TNFα, IL-1β, and SOD2 (data not shown). Therefore, we examined the involvement of NF-κB in the potentiation of the TNFα and IL-1β expression mediated by SOD2 knockdown. Consequently, a luciferase assay showed that the NF-κB activity was significantly increased 1.5 and 3 h after treatment with LPS (Fig. 8*A*). Additionally, SOD2 knockdown slightly increased the NF-κB activity induced by LPS at 1.5 h; however, the activity was predominantly potentiated at the 3-h time point (Fig. 8*A*). Moreover, the LPS-induced binding of NF-κB to its response element was largely enhanced by SOD2 knockdown (Fig. 8*B*). Therefore, it is

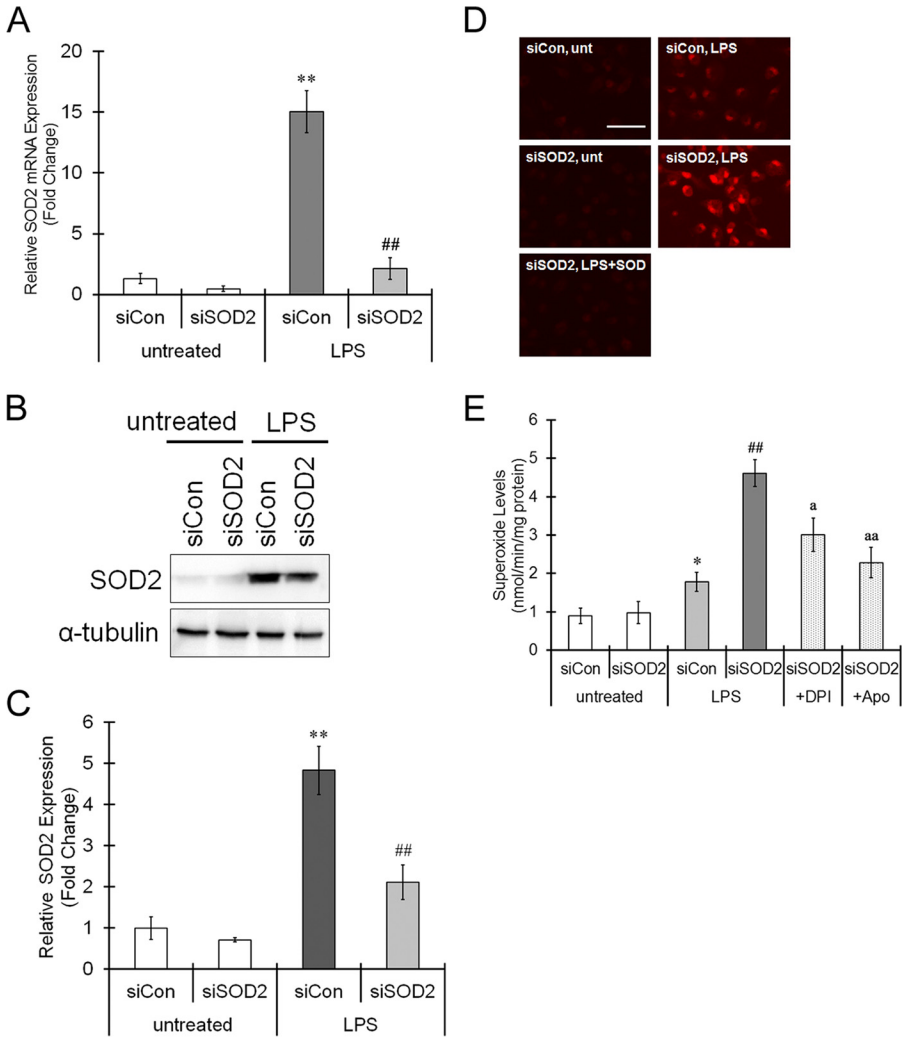

FIGURE 5. **Effects of SOD2 knockdown on ROS production in activated microglia.** After transfection of SOD2 siRNA (*siSOD2*) or control siRNA (*siCon*) into primary microglia, the cells were incubated for 24 h and then further incubated in the presence or absence of 10 ng/ml LPS for up to 24 h. *A*, after 6 h of incubation, the mRNA levels of SOD2 were measured using real-time PCR and are represented as -fold changes from the levels measured in untreated cells. The values represent the mean ± S.E. (*error bars*) of six separate experiments. The data were compared using Student's *t* test with Holm's corrections for multiple comparisons. **, $p < 0.01$ *versus* the untreated group carrying control siRNA. ##, $p < 0.01$ *versus* the LPS-treated group carrying control siRNA. *B*, after incubation for 24 h, SOD2 proteins in the cell lysates were detected using immunoblotting. The results are representative of four independent experiments. *C*, the band intensity represented in *B* was determined using the ImageJ software program. The values represent the mean ± S.E. of four separate experiments. The data were compared using Student's *t* test with Holm's corrections for multiple comparisons. **, $p < 0.01$ *versus* the untreated group carrying control siRNA; ##, $p < 0.01$ *versus* the LPS-treated group carrying control siRNA. *D*, representative images of ROS inside cells measured using DHE 3 h after stimulation with 10 ng/ml LPS. A cell membrane-permeable SOD, SOD-PEG, was added just before the addition of LPS, at a final concentration of 100 units/ml. The results are representative of five independent experiments. *Bar*, 100 μm. *E*, SOD2 siRNAs (*siSOD2*) or their control siRNAs (*siCon*) were transfected into primary microglia. After 24 h of incubation, the cells were pretreated with the NADPH oxidase inhibitors, 1 μM DPI or 100 μM apocynin (*Apo*), and then cultured in the presence or absence of 10 ng/ml LPS for 3 h. The amount of superoxide in the culture media was measured using acetylated cytochrome *c*. The values represent the mean ± S.E. of four separate experiments. The data were analyzed using one-way ANOVA, followed by Student's *t* test or Dunnett's test. The Bonferroni method was used to correct for multiple comparisons. *, $p < 0.05$ *versus* the untreated group carrying control siRNA; ##, $p < 0.01$ *versus* the LPS-treated group carrying control siRNA. *a*, $p < 0.05$; *aa*, $p < 0.01$ *versus* the LPS-treated group carrying SOD2 siRNA.

suggested that the up-regulation of SOD2 suppresses the NF-κB activation induced by ROS, followed by the attenuation of microglial activation.

SOD2 Expression in an in Vivo Mouse Model of Neuroinflammation—Male ICR mice were administered LPS intraventricularly to produce a simple model of neuroinflammation. Intraventricular treatment with LPS resulted in an increased mRNA expression of TNFα and IL-1β, confirming the presence of inflammation in the brain (Fig. 9*A*). In addition, SOD2 mRNA was increased by LPS in the cortex of the mice (Fig. 9*B*). Therefore, activated microglia might increase the expression of SOD2 *in vivo*.

Discussion

In this study, the stimulation of microglial TLR4 by LPS increased the levels of proinflammatory cytokines and chemokines as well as the superoxide-scavenging enzyme, SOD2. TLR family ligands other than LPS, such as poly(I:C), PGN, and CpG DNA, also up-regulated the SOD2 expression, indicating the existence of a common mechanism among members of the TLR family for elevating the SOD2 expression in microglia. Downstream of TLR stimulation, adaptor proteins, such as MyD88 and TRIF, are recruited to the intracellular domain of TLRs, followed by the activation of kinases, including the IRAK family

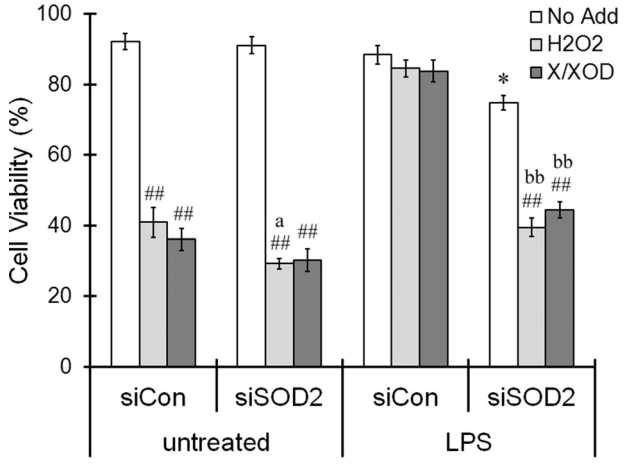

FIGURE 6. **Oxidative stress tolerance in the microglia with an increased expression of SOD2.** Twenty-four hours after transfection with SOD2 siRNA (*siSOD2*) or control siRNA (*siCon*), primary microglia were treated with 10 ng/ml LPS for 24 h. The cells were then administered oxidants, 300 μM hydrogen peroxide (H_2O_2) or 100 μM xanthine plus 30 milliunits/ml xanthine oxidase (*X/XOD*) for 24 h, and cell viability was assessed based on leakage of lactate dehydrogenase. The values represent the mean ± S.E. (*error bars*) of six separate experiments. The data were analyzed using one-way ANOVA, followed by Student's *t* test or Dunnett's test. The Bonferroni method was used to correct for multiple comparisons. *, $p < 0.05$ *versus* the LPS-treated group carrying control siRNA with no additional oxidant treatment (*No Add*). ##, $p < 0.01$ *versus* each group with no additional oxidant treatment. *a*, $p < 0.05$ *versus* the untreated group carrying control siRNA with oxidant treatment. *bb*, $p < 0.01$ *versus* the LPS-treated group carrying control siRNA with oxidant treatment.

(35). Subsequently, the transcription factor NF-κB is activated by the phosphorylation and degradation of IκB. In addition, AP-1 is activated via the MAPK pathway mediated by p38 and JNK. In the current study, the increased expression of SOD2 was suppressed by inhibitors of both NF-κB and AP-1, and LPS activated the SOD2 promoter, including the NF-κB and AP-1 binding sequences. Therefore, it is considered that NF-κB and AP-1 are involved in the transcriptional activation of SOD2 in microglia and that the SOD2 expression may be constantly elevated in microglia under inflammatory conditions. A mouse model of neuroinflammation also showed an increased expression of TNFα and IL-1β, as well as SOD2. Moreover, an increased expression of SOD2 in response to LPS was observed only in microglia, not in neurons or astrocytes. Some reports have indicated that TLR4 is not fully expressed in neurons and astrocytes (44, 45), and these cells thus cannot directly respond to LPS, consistent with our results. The increased SOD2 expression noted in the mouse model of neuroinflammation might reflect the microglial expression of SOD2.

Because ROS production was largely increased by SOD2 knockdown in the activated microglia, SOD2 can be considered to negatively regulate ROS production by microglia. Superoxide is primarily generated in mammalian cells and then converted into hydrogen peroxide and hydroxyl radicals. Therefore, the overall levels of ROS can be effectively reduced by eliminating superoxide. Activated microglia produce superoxide predominantly from NADPH oxidase, although ROS generation from mitochondria has also been reported (10, 11). Of note, once ROS are generated anywhere within cells, further ROS generation is induced via uncoupling of the mitochondrial respiratory chain, known as ROS-induced ROS release (46). In this regard, the regulation of ROS generation by mitochondria is important for controlling the redox balance. In another case, West *et al.* (47) recently reported that stimulation of TLR1, -2, or -4 in macrophages elicited mitochondrial ROS production via the TRAF6-ECSIT pathway, resulting in bacterial killing. Because SOD2 is localized in mitochondria and increases in the ROS levels induced by SOD2 knockdown were partially abolished by the inhibitors of NADPH oxidase in the present study, ROS are considered to be generated in activated microglia primarily from NADPH oxidase and secondarily from ROS-induced ROS release within the mitochondria.

Cell death was not induced by hydrogen peroxide or xanthine/xanthine oxidase in the microglia treated with LPS, indicating that activated microglia show higher tolerance to oxidative stress than microglia in the resting state. Because activated microglia with SOD2 knockdown were injured by hydrogen peroxide and xanthine/xanthine oxidase, it appears that treatment with LPS up-regulates SOD2 expression, which protects cells form subsequent challenges of oxidative stress induced by hydrogen peroxide or xanthine/xanthine oxidase. Activated microglia generate massive amounts of ROS, which play an important (patho)physiological role in the removal of bacteria, whereas the oxidative stress condition elicited by microglia may potentially damage the microglia themselves. One of the major roles of the SOD2 elicited in activated microglia could be to protect the microglia from the oxidative stress that they generate as a defense against foreign organisms.

Interestingly, the expression of proinflammatory cytokines was increased in the activated microglia with SOD2 knockdown compared with the control siRNA-treated cells. Therefore, it is suggested that SOD2 in activated microglia might negatively regulate the expression of proinflammatory cytokines. In addition, treatment of microglia with LPS stimulated ROS production, and SOD2 knockdown potentiated the increases in ROS induced by LPS, whereas the inhibition of NADPH oxidase by DPI or apocynin largely suppressed ROS production in the microglia. DPI and apocynin also attenuated the LPS-induced expression of TNFα and IL-1β potentiated by the transfection of SOD2 siRNA. Therefore, the ROS levels in microglia correlate with the cytokine expression, suggesting that ROS might regulate the proinflammatory responses of microglia.

The expression of proinflammatory cytokines is tightly controlled by the transcription factor, NF-κB (35), and NF-κB is notably known to be activated by ROS (42, 43). Carboxyalkylpyrroles, the end products of lipid peroxidation, activate NF-κB via TLR2 stimulation and subsequent MyD88 recruitment (48). ROS inactivate phosphatases, after which kinases that are relatively activated, especially IKK, induce IκB phosphorylation and subsequent ubiquitination and degradation by proteasomes, followed by the translocation of released NF-κB into the nucleus and subsequent gene transcription (49). In this study, increased NF-κB activity was detected in the microglia treated with LPS, and this effect was enhanced by SOD2 knockdown. Therefore, SOD2 could be considered to negatively regulate the NF-κB activity by eliminating ROS. The mechanism by which microglia are activated under inflammatory conditions is well studied and involves pattern recognition receptors, such as TLRs, which recognize xenobiotics, followed by the

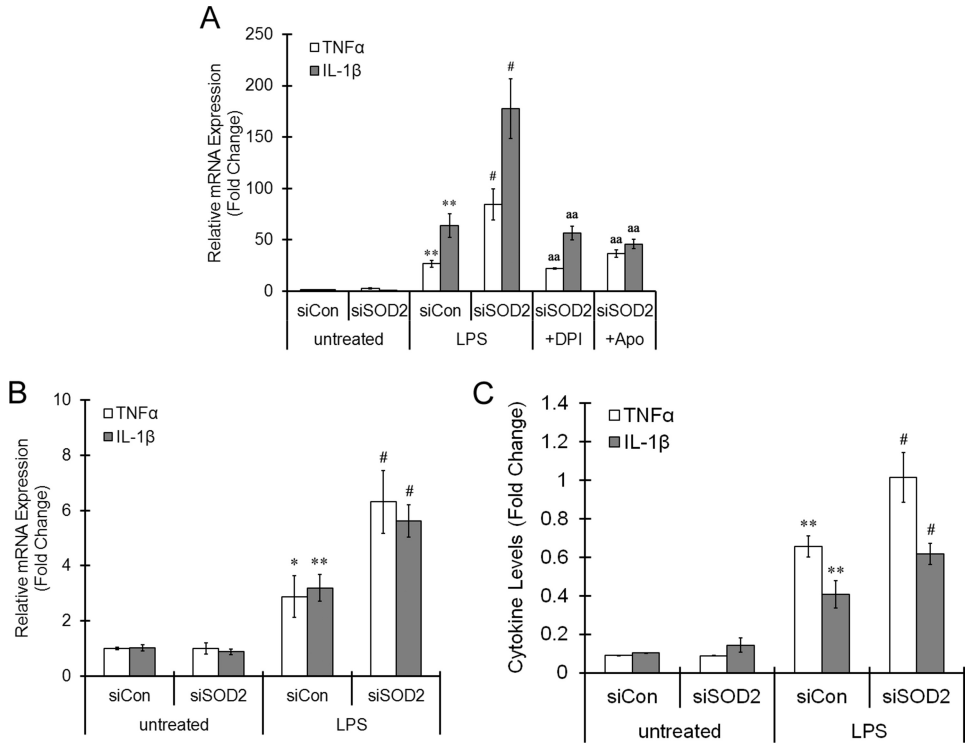

FIGURE 7. **Decreases in the proinflammatory cytokine expression mediated by SOD2 in activated microglia.** Rat primary microglia were transfected with SOD2 siRNA (siSOD2) or control siRNA (siCon) and then cultured for 24 h. The cells were pretreated with 1 μM DPI or 100 μM apocynin (*Apo*) and subsequently treated with LPS for 6 (*A*), 12 (*B*), and 24 h (*C*). The levels of TNFα and IL-1β mRNA were measured using real-time PCR (*A* and *B*), and the protein levels of TNFα and IL-1β in the culture media were quantified via ELISA (*C*). The values represent the mean ± S.E. (*error bars*) of five separate experiments. The data were analyzed using one-way ANOVA, followed by Student's *t* test or Dunnett's test. The Bonferroni method was used to correct for multiple comparisons. *, $p < 0.05$; **$p < 0.01$ *versus* the untreated group carrying control siRNA. #, $p < 0.05$; ##, $p < 0.01$ *versus* the LPS-treated group carrying control siRNA. *aa*, $p < 0.01$ *versus* the LPS-treated group carrying SOD2 siRNA.

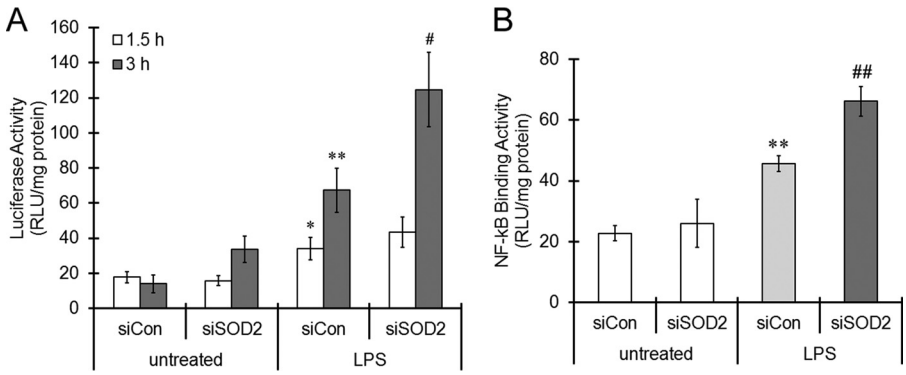

FIGURE 8. **Suppressive effects of SOD2 on the NF-κB transcriptional activity in activated microglia.** *A*, rat primary microglia were co-transfected with pNL3.2.NF-κB-RE and SOD2 siRNA (*siSOD2*) or control siRNA (*siCon*) and cultured for 24 h. After treatment with 10 ng/ml LPS for 3 or 1.5 h, the cells were lysed, and the luciferase activity was measured. *B*, after transfection with SOD2 siRNA or control siRNA, rat primary microglia were incubated for 24 h and then incubated for an additional 3 h with 10 ng/ml LPS. The nuclear fraction was extracted. The binding capacity of NF-κB to its response element was evaluated using an NF-κB (p65) transcription factor assay kit. The values are expressed as the mean ± S.E. (*error bars*) of 4–5 separate experiments. The data were compared using Student's *t* test with Holm's corrections for multiple comparisons. **, $p < 0.01$ *versus* the untreated cells carrying control siRNA. #, $p < 0.05$; ##, $p < 0.01$ *versus* the LPS-treated group carrying control siRNA.

activation of downstream signals (35). On the other hand, there are few reports about the physiological mechanisms that positively terminate microglial activation and neuroinflammation (*e.g.* the dopamine D2 receptor-αB-crystallin pathway has been investigated) (50). Our findings indicate that microglia up-regulate SOD2 during activation (at the beginning of inflammation), and the increased SOD2 subsequently inactivates microglia (terminating inflammation). Specifically, SOD2 may restrict microglial activation to the minimum extent necessary (Fig. 10). Because SOD2 was transcriptionally increased by NF-κB in activated microglia and SOD2 subsequently decreased the NF-κB activity to reduce the quantity of proinflammatory cytokines, the microglial production of proinflammatory cytokines may be regulated, at least in part, by "negative feedback" involving the NF-κB-SOD2 pathway (Fig. 10). In addition, dead cells contribute to inflammation by scattering their intracellular contents. Therefore, the suppression of microglial oxidative injury by SOD2 might also be involved in attenuating neuroinflammation. Because the excess or prolonged activation of microglia is known to induce various CNS

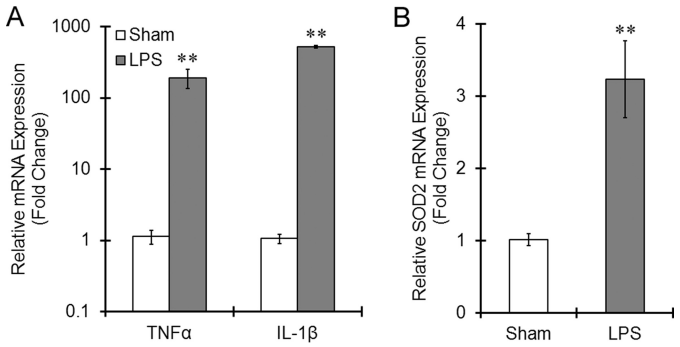

FIGURE 9. **Effects of the intraventricular administration of LPS on the SOD2 expression in the cerebral cortex of the mice.** Male ICR mice (8 weeks old) were administered 40 μg/kg LPS intraventricularly. After 3 h, the cerebral cortex was isolated, RNA was extracted, and cDNA was synthesized. The levels of TNFα and IL-1β (*A*) and SOD2 (*B*) mRNA were measured using real-time PCR and normalized to the β-actin mRNA levels, and the values for the treated samples were divided by those for the untreated samples to calculate the relative mRNA levels. The intraventricular administration of LPS resulted in an increased expression of TNFα and IL-1β, as well as SOD2, in the mice. The data were compared using Student's *t* test. The values represent the mean $\pm$ S.E. (*error bars*) of five separate experiments. **, $p < 0.01$ *versus* the sham-operated group.

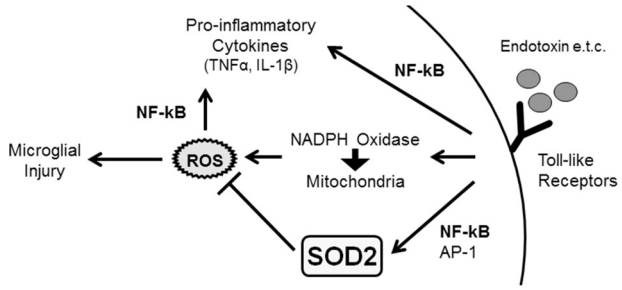

FIGURE 10. **Putative role of the SOD2 induced in activated microglia.** Mechanistic insight into the role of SOD2 up-regulation in activated microglia. SOD2 is up-regulated downstream of TLRs via NF-κB and AP-1. Increased SOD2 scavenges ROS, not only to protect microglia from the oxidative stress induced under inflammatory conditions, but also to decrease the inflammatory cytokine expression by suppressing the NF-κB activity. SOD2 regulates the microglial activity via an NF-κB-mediated feedback loop, terminating microglial activation.

disorders, including neurodegenerative diseases and epilepsy (1–5), this mechanism for controlling the activity of microglia may effectively maintain immune homeostasis in the CNS.

Polymorphisms of SOD2 have been reported to be associated with the development of neurodegenerative diseases, such as Alzheimer disease (51) and Parkinson disease (52, 53), as well as psychiatric disorders, such as schizophrenia (54), depression (55), and bipolar disorder (56). Notably, neuroinflammation is closely linked to the onset and/or development of these CNS diseases (1–5). Considering these reports and our findings, SOD2 mutations may induce diverse CNS diseases due to excessive or prolonged microglial activation and subsequent neuroinflammation. Further research is needed to reveal the relationships between the SOD2 expressed in microglia and CNS disorders mediated by neuroinflammation.

In conclusion, in this study, SOD2 was up-regulated downstream of TLRs in activated microglia. Increased SOD2 conferred oxidative stress tolerance on microglia, and, concomitant with this process, SOD2 decreased the proinflammatory cytokine expression by attenuating the NF-κB activation mediated by ROS, followed by the termination of microglial activation. SOD2 is therefore considered to regulate the immune system in the CNS by acting as a switch to control microglial activation/inactivation.

Author Contributions—Y. I. and T. Y. designed the research and wrote the paper. Y. I., T. T., and A. I. conducted the majority of experiments. K. I. carried out the culture of primary neurons and prepared the mouse model of neuroinflammation. All authors commented on the manuscript.

Acknowledgment—We thank Dr. Beth Stevens (Harvard Medical School) for a critical review of the manuscript.

References

1. Marinova-Mutafchieva, L., Sadeghian, M., Broom, L., Davis, J. B., Medhurst, A. D., and Dexter, D. T. (2009) Relationship between microglial activation and dopaminergic neuronal loss in the substantia nigra: a time course study in a 6-hydroxydopamine model of Parkinson's disease. *J. Neurochem.* **110,** 966–975
2. Hickman, S. E., Allison, E. K., and El Khoury, J. (2008) Microglial dysfunction and defective β-amyloid clearance pathways in aging Alzheimer's disease mice. *J. Neurosci.* **28,** 8354–8360
3. Wang, Y. C., Lin, S., and Yang, Q. W. (2011) Toll-like receptors in cerebral ischemic inflammatory injury. *J. Neuroinflammation* **8,** 134
4. Najjar, S., Pearlman, D. M., Alper, K., Najjar, A., and Devinsky, O. (2013) Neuroinflammation and psychiatric illness. *J. Neuroinflammation* **10,** 43
5. Xanthos, D. N., and Sandkühler, J. (2014) Neurogenic neuroinflammation: inflammatory CNS reactions in response to neuronal activity. *Nat. Rev. Neurosci.* **15,** 43–53
6. Block, M. L., and Hong, J. S. (2005) Microglia and inflammation-mediated neurodegeneration: multiple triggers with a common mechanism. *Prog. Neurobiol.* **76,** 77–98
7. Bedard, K., and Krause, K. H. (2007) The NOX family of ROS-generating NADPH oxidases: physiology and pathophysiology. *Physiol. Rev.* **87,** 245–313
8. Petry, A., Weitnauer, M., and Görlach, A. (2010) Receptor activation of NADPH oxidases. *Antioxid. Redox Signal.* **13,** 467–487
9. DeChatelet, L. R., McPhail, L. C., Mullikin, D., and McCall, C. E. (1975) An isotopic assay for NADPH oxidase activity and some characteristics of the enzyme from human polymorphonuclear leukocytes. *J. Clin. Invest.* **55,** 714–721
10. Hu, Z., Yu, F., Gong, P., Qiu, Y., Zhou, W., Cui, Y., Li, J., and Chen, H. (2014) Subneurotoxic copper(II)-induced NF-κB-dependent microglial activation is associated with mitochondrial ROS. *Toxicol. Appl. Pharmacol.* **276,** 95–103
11. Volobouéva, L. A., Emery, J. F., Sun, X., and Giffard, R. G. (2013) Inflammatory response of microglial BV-2 cells includes a glycolytic shift and is modulated by mitochondrial glucose-regulated protein 75/mortalin. *FEBS Lett.* **587,** 756–762
12. Naik, E., and Dixit, V. M. (2011) Mitochondrial reactive oxygen species drive proinflammatory cytokine production. *J. Exp. Med.* **208,** 417–420
13. Wang, T., Qin, L., Liu, B., Liu, Y., Wilson, B., Eling, T. E., Langenbach, R., Taniura, S., and Hong, J. S. (2004) Role of reactive oxygen species in LPS-induced production of prostaglandin E2 in microglia. *J. Neurochem.* **88,** 939–947
14. Pawate, S., Shen, Q., Fan, F., and Bhat, N. R. (2004) Redox regulation of glial inflammatory response to lipopolysaccharide and interferongamma. *J. Neurosci. Res.* **77,** 540–551
15. Qin, L., Liu, Y., Wang, T., Wei, S. J., Block, M. L., Wilson, B., Liu, B., and Hong, J. S. (2004) NADPH oxidase mediates lipopolysaccharide-induced neurotoxicity and proinflammatory gene expression in activated microglia. *J. Biol. Chem.* **279,** 1415–1421
16. Chéret, C., Gervais, A., Lelli, A., Colin, C., Amar, L., Ravassard, P., Mallet, J., Cumano, A., Krause, K. H., and Mallat, M. (2008) Neurotoxic activation of microglia is promoted by a nox1-dependent NADPH oxidase. *J. Neu-*

rosci. **28,** 12039–12051
17. Park, H. S., Jung, H. Y., Park, E. Y., Kim, J., Lee, W. J., and Bae, Y. S. (2004) Cutting edge: direct interaction of TLR4 with NAD(P)H oxidase 4 isozyme is essential for lipopolysaccharide-induced production of reactive oxygen species and activation of NF-κB. *J. Immunol.* **173,** 3589–3593
18. Qin, L., Liu, Y., Hong, J. S., and Crews, F. T. (2013) NADPH oxidase and aging drive microglial activation, oxidative stress, and dopaminergic neurodegeneration following systemic LPS administration. *Glia* **61,** 855–868
19. Egger, T., Schuligoi, R., Wintersperger, A., Amann, R., Malle, E., and Sattler, W. (2003) Vitamin E (α-tocopherol) attenuates cyclo-oxygenase 2 transcription and synthesis in immortalized murine BV-2 microglia. *Biochem. J.* **370,** 459–467
20. Heppner, F. L., Roth, K., Nitsch, R., and Hailer, N. P. (1998) Vitamin E induces ramification and downregulation of adhesion molecules in cultured microglial cells. *Glia* **22,** 180–188
21. Godbout, J. P., Berg, B. M., Kelley, K. W., and Johnson, R. W. (2004) α-Tocopherol reduces lipopolysaccharide-induced peroxide radical formation and interleukin-6 secretion in primary murine microglia and in brain. *J. Neuroimmunol.* **149,** 101–109
22. Li, Y., Liu, L., Barger, S. W., Mrak, R. E., and Griffin, W. S. (2001) Vitamin E suppression of microglial activation is neuroprotective. *J. Neurosci. Res.* **66,** 163–170
23. Sugaya, K., Chou, S., Xu, S. J., and McKinney, M. (1998) Indicators of glial activation and brain oxidative stress after intraventricular infusion of endotoxin. *Brain Res. Mol. Brain Res.* **58,** 1–9
24. Kramer, B. C., Yabut, J. A., Cheong, J., JnoBaptiste, R., Robakis, T., Olanow, C. W., and Mytilineou, C. (2002) Lipopolysaccharide prevents cell death caused by glutathione depletion: possible mechanisms of protection. *Neuroscience* **114,** 361–372
25. Kaneko, Y. S., Ota, A., Nakashima, A., Mori, K., Nagatsu, I., and Nagatsu, T. (2012) Regulation of oxidative stress in long-lived lipopolysaccharide-activated microglia. *Clin. Exp. Pharmacol. Physiol.* **39,** 599–607
26. Sugaya, K., Chouinard, M. L., and McKinney, M. (1997) Induction of manganese superoxide dismutase in BV-2 microglial cells. *Neuroreport* **8,** 3547–3551
27. Chen, X., Choi, I. Y., Chang, T. S., Noh, Y. H., Shin, C. Y., Wu, C. F., Ko, K. H., and Kim, W. K. (2009) Pretreatment with interferon-γ protects microglia from oxidative stress via up-regulation of Mn-SOD. *Free Radic. Biol. Med.* **46,** 1204–1210
28. Ishihara, Y., Itoh, K., Ishida, A., and Yamazaki, T. (2015) Selective estrogen-receptor modulators suppress microglial activation and neuronal cell death via an estrogen receptor-dependent pathway. *J. Steroid Biochem. Mol. Biol.* **145,** 85–93
29. Ishihara, Y., Kawami, T., Ishida, A., and Yamazaki, T. (2012) Tributyltin induces oxidative stress and neuronal injury by inhibiting glutathione *S*-transferase in rat organotypic hippocampal slice cultures. *Neurochem. Int.* **60,** 782–790
30. Itoh, K., Kawamura, H., and Asou, H. (1992) A novel monoclonal antibody against carbohydrates of L1 cell adhesion molecule causes an influx of calcium in cultured cortical neurons. *Brain Res.* **580,** 233–240
31. Takemoto, T., Ishihara, Y., Ishida, A., and Yamazaki, T. (2015) Neuroprotection elicited by nerve growth factor and brain-derived neurotrophic factor released from astrocytes in response to methylmercury. *Environ. Toxicol. Pharmacol.* **40,** 199–205
32. Ishihara, Y., Fujitani, N., Kawami, T., Adachi, C., Ishida, A., and Yamazaki, T. (2014) Suppressive effects of 17β-estradiol on tributyltin-induced neuronal injury via Akt activation and subsequent attenuation of oxidative stress. *Life Sci.* **99,** 24–30
33. Ishihara, Y., Shiba, D., and Shimamoto, N. (2006) Enhancement of DMNQ-induced hepatocyte toxicity by cytochrome P450 inhibition. *Toxicol. Appl. Pharmacol.* **214,** 109–117
34. Ishihara, Y., Ito, F., and Shimamoto, N. (2011) Increased expression of c-Fos by extracellular signal-regulated kinase activation under sustained oxidative stress elicits BimEL upregulation and hepatocyte apoptosis. *FEBS J.* **278,** 1873–1881
35. Kawai, T., and Akira, S. (2010) The role of pattern-recognition receptors in innate immunity: update on Toll-like receptors. *Nat. Immunol.* **11,** 373–384
36. Kiningham, K. K., Xu, Y., Daosukho, C., Popova, B., and St Clair, D. K. (2001) Nuclear factor κB-dependent mechanisms coordinate the synergistic effect of PMA and cytokines on the induction of superoxide dismutase 2. *Biochem. J.* **353,** 147–156
37. Xu, Y., Kiningham, K. K., Devalaraja, M. N., Yeh, C. C., Majima, H., Kasarskis, E. J., and St Clair, D. K. (1999) An intronic NF-κB element is essential for induction of the human manganese superoxide dismutase gene by tumor necrosis factor-α and interleukin-1β. *DNA Cell Biol.* **18,** 709–722
38. Kairisalo, M., Korhonen, L., Blomgren, K., and Lindholm, D. (2007) X-linked inhibitor of apoptosis protein increases mitochondrial antioxidants through NF-κB activation. *Biochem. Biophys. Res. Commun.* **364,** 138–144
39. Kiningham, K. K., Cardozo, Z. A., Cook, C., Cole, M. P., Stewart, J. C., Tassone, M., Coleman, M. C., and Spitz, D. R. (2008) All-*trans*-retinoic acid induces manganese superoxide dismutase in human neuroblastoma through NF-κB. *Free Radic. Biol. Med.* **44,** 1610–1616
40. Borrello, S., and Demple, B. (1997) NF kappa B-independent transcriptional induction of the human manganous superoxide dismutase gene. *Arch. Biochem. Biophys.* **348,** 289–294
41. Kaneko, M., Takahashi, T., Niinuma, Y., and Nomura, Y. (2004) Manganese superoxide dismutase is induced by endoplasmic reticulum stress through IRE1-mediated nuclear factor (NF)-κB and AP-1 activation. *Biol. Pharm. Bull.* **27,** 1202–1206
42. Warner, B. B., Stuart, L., Gebb, S., and Wispé, J. R. (1996) Redox regulation of manganese superoxide dismutase. *Am. J. Physiol.* **271,** L150–L158
43. Das, K. C., Lewis-Molock, Y., and White, C. W. (1995) Activation of NF-κB and elevation of MnSOD gene expression by thiol reducing agents in lung adenocarcinoma (A549) cells. *Am. J. Physiol.* **269,** L588–L602
44. Chakravarty, S., and Herkenham, M. (2005) Toll-like receptor 4 on nonhematopoietic cells sustains CNS inflammation during endotoxemia, independent of systemic cytokines. *J. Neurosci.* **25,** 1788–1796
45. Lehnardt, S., Massillon, L., Follett, P., Jensen, F. E., Ratan, R., Rosenberg, P. A., Volpe, J. J., and Vartanian, T. (2003) Activation of innate immunity in the CNS triggers neurodegeneration through a Toll-like receptor 4-dependent pathway. *Proc. Natl. Acad. Sci. U.S.A.* **100,** 8514–8519
46. Zorov, D. B., Juhaszova, M., and Sollott, S. J. (2014) Mitochondrial reactive oxygen species (ROS) and ROS-induced ROS release. *Physiol. Rev.* **94,** 909–950
47. West, A. P., Brodsky, I. E., Rahner, C., Woo, D. K., Erdjument-Bromage, H., Tempst, P., Walsh, M. C., Choi, Y., Shadel, G. S., and Ghosh, S. (2011) TLR signalling augments macrophage bactericidal activity through mitochondrial ROS. *Nature* **472,** 476–480
48. West, X. Z., Malinin, N. L., Merkulova, A. A., Tischenko, M., Kerr, B. A., Borden, E. C., Podrez, E. A., Salomon, R. G., and Byzova, T. V. (2010) Oxidative stress induces angiogenesis by activating TLR2 with novel endogenous ligands. *Nature* **467,** 972–976
49. Jin Jung, K., Hyun Kim, D., Kyeong Lee, E., Woo Song, C., Pal Yu, B., and Young Chung, H. (2013) Oxidative stress induces inactivation of protein phosphatase 2A, promoting proinflammatory NF-κB in aged rat kidney. *Free Radic. Biol. Med.* **61,** 206–217
50. Shao, W., Zhang, S. Z., Tang, M., Zhang, X. H., Zhou, Z., Yin, Y. Q., Zhou, Q. B., Huang, Y. Y., Liu, Y. J., Wawrousek, E., Chen, T., Li, S. B., Xu, M., Zhou, J. N., Hu, G., and Zhou, J. W. (2013) Suppression of neuroinflammation by astrocytic dopamine D2 receptors via αB-crystallin. *Nature* **494,** 90–94
51. Wiener, H. W., Perry, R. T., Chen, Z., Harrell, L. E., and Go, R. C. (2007) A polymorphism in SOD2 is associated with development of Alzheimer's disease. *Genes Brain Behav.* **6,** 770–775
52. Wang, V., Chen, S. Y., Chuang, T. C., Shan, D. E., Soong, B. W., and Kao, M. C. (2010) Val-9Ala and Ile+58Thr polymorphism of MnSOD in Parkinson's disease. *Clin. Biochem.* **43,** 979–982
53. Shimoda-Matsubayashi, S., Matsumine, H., Kobayashi, T., Nakagawa-Hattori, Y., Shimizu, Y., and Mizuno, Y. (1996) Structural dimorphism in the mitochondrial targeting sequence in the human manganese superoxide dismutase gene: a predictive evidence for conformational change to influence mitochondrial transport and a study of allelic association in Parkinson's disease. *Biochem. Biophys. Res. Commun.* **226,** 561–565

54. Akyol, O., Yanik, M., Elyas, H., Namli, M., Canatan, H., Akin, H., Yuce, H., Yilmaz, H. R., Tutkun, H., Sogut, S., Herken, H., Ozyurt, H., Savas, H. A., and Zoroglu, S. S. (2005) Association between Ala-9Val polymorphism of Mn-SOD gene and schizophrenia. *Prog. Neuropsychopharmacol. Biol. Psychiatry* **29,** 123–131
55. Gałecki, P., Smigielski, J., Florkowski, A., Bobińska, K., Pietras, T., and Szemraj, J. (2010) Analysis of two polymorphisms of the manganese superoxide dismutase gene (Ile-58Thr and Ala-9Val) in patients with recurrent depressive disorder. *Psychiatry Res.* **179,** 43–46
56. Fullerton, J. M., Tiwari, Y., Agahi, G., Heath, A., Berk, M., Mitchell, P. B., and Schofield, P. R. (2010) Assessing oxidative pathway genes as risk factors for bipolar disorder. *Bipolar Disord.* **12,** 550–556

Dual Role of Superoxide Dismutase 2 Induced in Activated Microglia: OXIDATIVE STRESS TOLERANCE AND CONVERGENCE OF INFLAMMATORY RESPONSES

Yasuhiro Ishihara, Takuya Takemoto, Kouichi Itoh, Atsuhiko Ishida and Takeshi Yamazaki

J. Biol. Chem. 2015, 290:22805-22817.
doi: 10.1074/jbc.M115.659151 originally published online July 31, 2015